# The model of dynamics of multispan flexible rotor on active magnetic bearings applied for diagnostics

Viktor Ovchinnikov, Mikhail Nikolaev [a], Vasily Litvinov

Research Institute of Mechanics Lobachevsky State University of Nizhny Novgorod, Russia
[a] minick@mech.unn.ru

*Abstract*— **The paper presents a model of dynamics of multispan flexible rotor on active magnetic bearings (AMB) applied for composing of diagnostic characters of malfunctions.**

## I. INTRODUCTION

One of strongly developed lines of investigation of electromagnetic suspension is application of active magnetic bearings (AMB) to support complex flexible rotors of big size and weight, for example, in high-temperature gas-cooled nuclear power plants [1] or in wind power plants [2,3]. Such multispan flexible heterogeneous rotors meet the criteria formulated in [4], which describe complex unique system. Such rotors combine manifold revolving machines. Each AMB has its own control system interacting with other bearings' systems via the rotor. Numerous forces influencing the rotor excite several rotor vibration modes at once which, when combined, could lead to substantially different patterns of movement of various rotor parts. Thus, the system as a whole is completely nonlinear.

Application of the model of dynamics of multispan flexible rotor on AMB for diagnostics requires that during design and commissioning operations the research of dynamics of a malfunctioning rotor is conducted and diagnostic characters, or signatures, of such malfunctions are defined. Using measurable parameters that reflect the dynamics of such signatures, the framework is created that allows automatic detection of the malfunctions. This framework is included in diagnostic system of multispan flexible rotor on AMB running in operation modes. Therefore, the developed model should be fitting for computation of the rotor dynamics both in normal and in emergency operation modes taking into account structural deviations of design factors from their nominal values. It should also allow accounting for external influences, e.g. from seismic disturbances or hurricane winds if the rotor is a part of wind power plant.

## II. FUNDAMENTAL MODEL CHARACTERISTICS

To conduct the research needed both for designing and for operation such rotor systems we have composed the model of dynamics of flexible heterogeneous multispan rotor on AMB which is comprised by the mechanical model, the models of forces of various nature, the model of control system. The mechanical model is based on equations and results of studying of dynamics of flexible rotors [5]. Majority of dynamics problems take the rotor as elastic heterogeneous rod with piecewise characteristics. Its movements could be divided in for types of oscillations: as solid body, elastic torsional vibrations, elastic longitudinal and bending vibrations. For small oscillations of straight bars elastic torsional, longitudinal and bending oscillations could be considered independent. Specifics of dynamics of the rotor on AMB are determined by bending oscillations, therefore those bending oscillations are the main subject for this paper.

### *A. The mechanical model*

In the mechanical model of the rotor Cartesian coordinate system $0xyz$ is used. $0x$ axis is taken as vertical one coinciding with the rotation axis of the unstrained rotor. For composing the mechanical model the rotor is divided in series of interconnected homogeneous round sectors. For description of bending oscillations of sections the Timoshenko model of beam [6] is used, according to which the equations defining the dynamics of the rotor are

$$\begin{aligned} &\frac{\partial Q_y}{\partial x} = m\frac{\partial^2 U_y}{\partial t^2} - q_y, \\ &\frac{\partial M_z}{\partial x} = -Q_y + \rho I\frac{\partial^2 \Theta_z}{\partial t^2} - \mu_z, \\ &\frac{\partial \Theta_z}{\partial x} = \frac{1}{EI}M_z, \quad \frac{\partial U_y}{\partial x} = \Theta_z + \frac{1}{Gfr^*}Q_y. \end{aligned} \tag{1}$$

Here $U_y(x,t)$, $\Theta_z(x,t)$ describe linear and angular motions of the rotor along the $0y$ axis, $M_z(x,t)$, $Q_y(x,t)$ describe inner torques and intersecting stresses in the cross-section of the rotor. $q_y$, $\mu_z$ are distributed force and torque, respectively. $E$, $\nu$, $G=E/(2(1+\nu))$ are modulus of elasticity, Poisson ratio and rigidity modulus; $\rho$ is the density of rotor's material; $f$, $I$ are area of normal section and axial moment of inertia of a sector. $m$ is linear mass of a sector; $r^*$ is the coefficient for taking into account irregularity of tangential stress over normal section of a sector.

To combine the sectors in the integral mechanical model three types of connections are utilized: rigid, elastic and support. $U_y(x,t)$, $\Theta_z(x,t)$ and $M_z(x,t)$ are continuous at rigid connections and at support points. $Q_y(x,t)$ is continuous at rigid connections but is disconnected at the support points with jump equal to support reaction force. In the elastic connection section all forces and torques are continuous.

Equations (1) define bending vibrations along the $0y$ axis; similar ones could be composed for vibrations along the $0z$

axis, which will be characterized by $U_z(x,t)$, $\Theta_y(x,t)$, $M_y(x,t)$, $Q_z(x,t)$.

To transition to the discrete model of the rotor characteristic functions are expanded into series of the eigenmodes $U_k(x)$, $\Theta_k(x)$, $M_k(x)$, $Q_k(x)$. For the movements the expansion is written as follows:

$$U_y = \sum_{k=1}^{K} a_k(t)U_k(x), \quad U_z = \sum_{k=1}^{K} b_k(t)U_k(x), \qquad (2)$$

Here $K$ is the amount of eigenmodes taken into account.

Let us define $\boldsymbol{a}=\{a_k(t)\}$, $\boldsymbol{b}=\{b_k(t)\}$ as $K$-dimensioned vectors of generalized coordinates with components being functions of time $a_k(t)$ and $b_k(t)$ from expansion (2). Similar forms are used for functions describing rotation angles, torques and intersection stresses.

Choice of the basis is determined by the problem being solved. For calculation of dynamics of elastic structures in the presence of nonlinear interlinks, eigenmodes of oscillations of an unsupported rotor plus rotor movements as a solid body could be used. For modelling of dynamics of a flexible heterogeneous rotor on AMB we used the eigenmodes of oscillations of a rotor with pivoting support in cross-sections of AMB plus the static deformation modes. In this case AMB control system is expected to generate the required control laws (including linear ones) of the control forces depending on rotor displacements, thus it is reasonable to use as basis the orthogonal forms of Eigen oscillations of the rotor with boundary conditions corresponding to rotor resting on elastic supports with rigidity $c_n$ at cross-sections $x = x_n$ where AMB are placed and with free ends ( $n = \overline{1,N}$ , $N$ is the amount of radial AMB*)*. For basis to be orthogonal and normalized the following equations stand:

$$\int_0^l (mU_kU_j + \rho I\Theta_k\Theta_j)dx = \begin{Bmatrix} 0, k \neq j \\ m_0, k = j \end{Bmatrix}; \qquad (3)$$

$$k, j = \overline{1,K},$$

Here $m_0$ is the mass of the rotor. Integration is done over the whole length of the rotor $l$.

The mechanical model of the rotor is composed for vectors of generalized coordinates. To derive the solving equations Lagrange equations of second kind are used.

After substitution of derived expressions to Lagrange equations and taking into account the properties of eigenmodes of oscillations the mathematical model of dynamics of the rotor along the 0$y$ axis is written as:

$$m_0 \frac{d^2\boldsymbol{a}}{dt^2} + m_0\boldsymbol{\Omega a} = \boldsymbol{R}_a. \qquad (4)$$

$\boldsymbol{\Omega} = diag(\omega_1^2, \omega_2^2, ..., \omega_K^2)$ is a $K$-th order diagonal matrix with elements being squares of the Eigen frequencies of the rotor.

The equation for the vector $\boldsymbol{b}$ describing the movements of the rotor in the second horizontal axis 0$z$ is similar.

Components of the vectors of generalized forces are defined in a standard way and, taking into account equations (1) and expansions (2), could be written as:

$$\boldsymbol{R}_a = \{R_a^k\}, R_a^k = \int_0^l \{q_y U_k(x) + \mu_z \Theta_k(x)\}dx, \; k = \overline{1,K}.$$

This expression is formally correct for concentrated actions as well: such actions could be described using delta-functions. The formulas for the most important forces that are accounted for in the mathematical model are presented below.

The rotor is held in the desired position by forces from radial AMB $F_n$ which depend on horizontal displacements of the rotor $d_n = U_y(x_n)$ in the cross-sections of AMB and on currents in the coils. By virtue of (2) the displacement vector $\boldsymbol{d} = \{d_n\}$ could be expressed as follows:

$$\boldsymbol{d} = \boldsymbol{H} \cdot \boldsymbol{a}, \quad \boldsymbol{H} = \{h_{nk}\}, \quad h_{nk} = U_k(x_n).$$

Knowing the displacement vector and the currents in the coils, it is possible to determine the forces vector $\boldsymbol{F} = \{F_n\}$. This vector could be expressed as the sum

$$\boldsymbol{F} = -\boldsymbol{c} \cdot \boldsymbol{d} + \boldsymbol{F}^*, \quad \boldsymbol{c} = diag(c_1, ..., c_N).$$

The first term of the force describes the reaction of elastic supports, which is already accounted for in the oscillation eigenmodes. Thus, we should only put the second term into the equations (4) as a generalized force, which could be expressed by the following formula:

$$\boldsymbol{R_a} = \boldsymbol{H}^T \cdot \boldsymbol{F}^* = \boldsymbol{C} \cdot \boldsymbol{a} + \boldsymbol{H}^T \cdot \boldsymbol{F}, \quad \boldsymbol{C} = \boldsymbol{H}^T \cdot \boldsymbol{c} \cdot \boldsymbol{H}.$$

Upper index “T” stands for transposition operation of the matrix.

The gyroscopic forces in the motion equations (1) are included via distributed torques:

$$\mu_z = -2\omega\rho I \frac{\partial\Theta_y}{\partial t}, \quad \mu_y = 2\omega\rho I \frac{\partial\Theta_z}{\partial t}, \quad q_y = q_z = 0.$$

Here $\omega = \dfrac{d\varphi}{dt}$ is the angular speed of the rotor, $\varphi$ is the rotation angle of the rotor. Based on (2) the vectors of the generalized forced are expanded as follows:

$$\boldsymbol{R}_a = 2\omega \cdot \boldsymbol{P} \cdot \frac{d\boldsymbol{b}}{dt}, \; \boldsymbol{P} = \{p_{kj}\},$$

$$p_{kj} = \int_0^l \rho I\Theta_k\Theta_j dx, \; k, j = \overline{1,K}.$$

The presence of imbalance in the rotor impacts its dynamics by a distributed force

$$q_y = \omega^2 m[e_1(x)\cos\varphi - e_2(x)\sin\varphi],$$

$$q_z = \omega^2 m[e_1(x)\sin\varphi + e_2(x)\cos\varphi], \quad \mu_z = \mu_y = 0.$$

Here $e_1(x)$, $e_2(x)$ describe the position of center of mass of normal section of the rotor relative to the rotation axis in the coordinate system attached to the rotor. The related vectors of generalized forces are:

$$\boldsymbol{R}_a = \omega^2[\boldsymbol{S}_1\cos\varphi - \boldsymbol{S}_2\sin\varphi], \quad \boldsymbol{S}_i = \{s_{ki}\},$$

$$s_{ki} = \int_0^l me_i(x)U_k(x)dx, \quad k = \overline{1,K}, \quad i = 1,2.$$

Similar method is used to express the generalized forces of other natures. For a vertically placed rotor the gravity force effect on lateral rotor movements in the motion equations could be expressed by the following distributed forces:

$$q_y = \frac{\partial Q_0 \Theta_z}{\partial x}, \quad q_z = -\frac{\partial Q_0 \Theta_y}{\partial x}, \quad \mu_z = \mu_y = 0.$$

Here $Q_0(x)$ is the axial static force impacting the rotor.

The electromagnetic forces in generator, exciter and motor, as well as gas dynamic forces in turbines, compressors and their shafts' labyrinth seals are modelled by attraction forces:

$$q_y = r_e U_y, \quad q_z = r_e U_z, \quad \mu_z = \mu_y = 0$$

and circulation forces:

$$q_y = r_v U_z, \quad q_z = -r_v U_y, \quad \mu_z = \mu_y = 0.$$

Here $r_e$, $r_v$ are coefficients which depend on the design and characteristics of aforementioned elements.

*B. Accounting for the inner damping*

One of the main factors considerably influencing dynamics of the rotor is energy dissipation caused by external and inner damping [5]. The forces from external viscous friction associated with the rotor interaction with surrounding gas depend on the rotor design and speed. The electromagnetic forces in AMB are similar in the damping effect but are far bigger by value, so accounting for the external damping does not considerably improve the accuracy of the numerical analysis of dynamics of the rotor.

The inner damping can have substantial destabilizing effect on dynamics of the rotor. Numerous studies [7] show that in quite wide range of frequencies (0-10000 Hz) the level of dissipation of energy in structural materials does not depend on speed of deformation, but rather on stress conditions, deformation level and material temperature. The structural damping in joints has similar properties. Currently there are numerous theories of the inner damping which, under certain conditions, allow for accounting for the key features of the process of inner energy dissipation. For that the dependency between tensor of deformation $\varepsilon$ and tensor of stress $\sigma$ during the oscillations (including nonlinear) is used: $\sigma=\sigma(\varepsilon)$. In the general case, this dependency is nonlinear and ambiguous (hysteresis-like). Universal models of such dependency are not developed yet. Most theories and models of inner energy dissipation which are verified by experiments are either very complex for practical applications or are aimed at a limited pool of particular problems (steady-state oscillations, fixed-frequency oscillations, linear problems) [8, 9]. As a result, for the inner damping accounting we chose a trade-off decision based on two assumptions: a) energy dissipation has substantial effect on the oscillations near the resonance frequencies when rotor is revolving on near-Eigen frequencies; b) fundamental effects on dynamics of oscillations are defined by level of energy dissipation in one oscillation period (hysteresis loop area), and detailed dependency of stress from deformation (hysteresis loop shape) is of second importance.

In the developed model of dynamics of a flexible heterogeneous rotor, the inner damping is accounted separately for all generalized coordinates. For each generalized coordinate phenomenological model of friction damping is used (Korchinsky model, Leonov and Bezpalko model) [10]. Presence of the inner damping in the material of the rotor leads to additional generalized force added to all motion equations for the generalized coordinate $q_i$. In the coordinate system attached to the rotor additional force is expressed as follows:

$$R_i = -r_i \chi |q_i|^{\alpha} sign \frac{dq_i}{dt}, \; i = \overline{1,K} \qquad (5)$$

Here $r_i$ is partial rigidity associated with the coordinate $q_i$; $\chi, \alpha$ are the coefficients defining the level of energy dissipation and type of dependency from oscillation amplitude.

During cyclic deformations having amplitude $\Delta q_i$ energy loss in the presence of force (5) is defined as

$$\Delta W = \frac{4 r_i \chi}{\alpha + 1} \Delta q_i^{\alpha+1}.$$

Total amount of vibrational energy is defined as $W = r_i (\Delta q_i)^2/2$ while relative energy loss is defined as

$$\psi = \Delta W / W = \frac{8\chi}{\alpha + 1} \Delta q_i^{\alpha-1}. \qquad (6)$$

The relation (6) along with the dependency between logarithmic decrement $\delta$ and relative loss $\psi$ ($\psi = 2\delta$) leads to possibility of finding the coefficients $\chi$ and $\alpha$ based on experimental data on the logarithmic decrements. It is worth noting that for $\alpha = 1$ expression (5) is reduced to the model of amplitude-independent damping, like in the model of the viscous friction. In this case:

$$R_i = -r_i \chi \Phi^*(q_i), \quad \Phi^*(q_i) = |q_i| sign \frac{dq_i}{dt}, \quad \chi = \delta / 2. \qquad (7)$$

Relation (7) is described as hysteresis loop shaped as triangle plotted on the axes $R_i$ and $q_i$.

The vectors of generalized coordinates $\boldsymbol{a}$, $\boldsymbol{b}$ (2) describe the movement of the rotor in the fixed global coordinate system $0xyz$. Vector $\boldsymbol{a}$ describes rotor movements along the axis $0y$, and vector $\boldsymbol{b}$ along the axis $0z$. To describe the deformations of the rotor it is convenient to use a coordinate system $0XYZ$ which is attached to the rotor. $0X$ axis of the moving coordinate system coincides with $0x$ axis of the fixed system; axes $0Y$ and $0Z$ have angle $\varphi$ against the axes $0y$ and $0z$ of the fixed system, respectively. Using this dependency of moving and fixed coordinate systems, for the vectors of generalized coordinates $\boldsymbol{A}$, $\boldsymbol{B}$ defining the rotor movements in the moving coordinate system along $0Y$ and $0Z$ axes, it could be put as follows:

$$\boldsymbol{A} = \boldsymbol{a} \cdot \cos\varphi + \boldsymbol{b} \cdot \sin\varphi; \quad \boldsymbol{B} = -\boldsymbol{a} \cdot \sin\varphi + \boldsymbol{b} \cdot \cos\varphi. \qquad (8)$$

To account for inner energy dissipation it is enough to add dissipation forces in the respective movement equations:

$$\boldsymbol{F}_A = -\frac{m_0}{2}\boldsymbol{D}_L \cdot \boldsymbol{\Omega} \cdot \boldsymbol{\Phi}(\boldsymbol{A}),$$
$$\boldsymbol{F}_B = -\frac{m_0}{2}\boldsymbol{D}_L \cdot \boldsymbol{\Omega} \cdot \boldsymbol{\Phi}(\boldsymbol{B}). \qquad (9)$$

Here $\boldsymbol{D}_L$ is the diagonal matrix of logarithmic decrements for the eigenmode oscillations. Expression $\boldsymbol{\Phi(q)}$ stands for the vector function with components defined by respective components of the vector $\boldsymbol{q}$:

$$\boldsymbol{\Phi} = \{\Phi_i\}, \quad \boldsymbol{q} = \{q_i\}, \quad \frac{d\boldsymbol{q}}{dt} = \left\{\frac{dq_i}{dt}\right\}, \quad \Phi_i = \Phi^*(q_i).$$

The generalized forces, when expressed in the moving coordinate system, are described as harmonic forces in the right-hand members of equations (5), as seen by inverse transformation of equations (9):

$$R_a = F_A \cos\varphi - F_B \sin\varphi,$$
$$R_b = F_A \sin\varphi + F_B \cos\varphi. \qquad (10)$$

Thus, to account for the inner energy dissipation in the rotor material and for the structural damping during the rotor deformations it is enough to add the generalized forces (10) to the mathematical model of dynamics of the rotor (4).

### *C. Accounting for the contact with a retainer bearing*

The machine of the rotor on AMB includes also mechanical retainer bearings, which prevent the rotor from colliding with structural elements of the stator (AMB magnets, guiding rigs in turbines and compressors, etc.) during emergency modes of operations (e.g. de-energizing of AMB) and during intensive external influences. Therefore, accounting for the rotor interaction with retainer bearings is essential for adequate modelling of dynamics of the rotor during emergencies. The model of retainer bearing is composed by analogy of the model of ring support of the tubing [11] with added specificity caused by rotation.

When analyzing physical processes taking place during interaction of an element of the rotor and the retainer bearing it is assumed that contact zone height is substantially smaller than the height of the rotor. In this case, contact zone size is negligible, and flat model of interaction of the rotor and the retainer bearing could be used. Relative position of the rotor and the retainer bearing is shown on Figure 1*a*. External surface of the rotor is described as a circle with radius $R$ and center in point $O$. The origin of the coordinate system $0xyz$ coincides with $O$. Contacting surface of the retainer bearing is modelled as a circle with radius $R_0$ and center at $S$. Relative position of the rotor and the bearing in equilibrium position is defined by the coordinates of $S$. Drawing of interaction of the rotor and the retainer bearing is shown on Figure 1*b*.

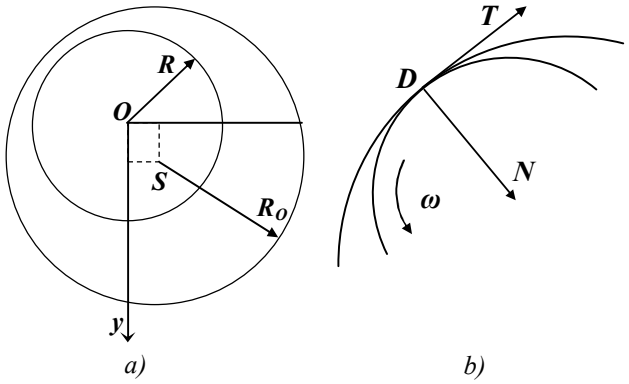


Figure 1. a) Relative position of the rotor and the retainer bearing; b) drawing of interaction of the rotor and the retainer bearing.

In mathematical formulation of the interaction process, it is assumed that linear size of contact area is substantially smaller than perimeter of the rotor circle. This allows using point model of the contact. In the contact point D tangents to the rotor surface and the retainer bearing surface coincide. When using elastic contact model, it could be seen that at the point D reaction force $\boldsymbol{N}$, which is normal to contacting surfaces, is proportional to deformation $\boldsymbol{d}$ of interacting elements:

$$\boldsymbol{N} = C \cdot \boldsymbol{d}. \qquad (11)$$

Here $C$ is rigidity of contact interaction. The normal force $\boldsymbol{N}$ effecting the rotor is directed from the point of contact to the center of the cross-section of the rotor.

At the point of contact there is also force $\boldsymbol{T}$ that is directed tangentially and its value is proportional to the reaction force and the friction coefficient $\mu$:

$$T = \mu \cdot N. \qquad (12)$$

Tangential force $\boldsymbol{T}$ affecting the rotor is directed oppositely to the tangential part of the movement speed of the point of contact.

Let us denote the maximum clearance between the rotor and the retainer bearing as $\Delta_0 = R_0 - R$. Minimum clearance happens when centers of the rotor and the bearing (points $O$ and $S$ on Figure 1) coincide. Relative position of the aforementioned centers in the original equilibrium position is described by the vector $\mathbf{S} = \overrightarrow{OS}$.

In the 2D coordinate system $0yz$ position of the center of the rotor during its movement is described by the vector $\boldsymbol{U}(t)$, and position of the center of the retainer bearing by the vector $\boldsymbol{S}$. In that case relative position of centers of the retainer bearing and the rotor is characterized by the vector

$$\boldsymbol{\Delta} = \boldsymbol{S} - \boldsymbol{U}(t). \qquad (13)$$

Modulus of this vector $\Delta$ equals current distance between the center of the retainer bearing and the center of the rotor. It is obvious that, when $\Delta<\Delta_0$, there is no contact between the rotor and the retainer bearing. In the other case contact happens, and the magnitude of it is defined by the relative deformation of the rotor and the bearing $d = \Delta - \Delta_0$.

The modulus of the reaction force (which is normal to contact surface) is defined by expression (11) and the force direction coincides with direction of the vector (13). Thusly,

when $d > 0$, the vector of normal contact force effecting the rotor from the retainer bearing could be written as follows:

$$\boldsymbol{N} = C \cdot d \cdot \boldsymbol{\Delta} / \Delta.$$

Value of tangential force effecting the rotor from the retainer bearing is defined by the expression (12) and its direction by the direction of the slip speed of the rotor in the contact point $\boldsymbol{V}_T$.

The total speed $\boldsymbol{V}_R(t)$ of the rotor at the contact point is composed by two parts: first is attributed to translational motion and is equal to the speed of the center of the rotor $\boldsymbol{V}(t)$, and second is attributed to relative movement caused by the rotor revolving around its axis with angular speed $\omega$:

$$\begin{aligned} &\boldsymbol{V}_R(t) = \boldsymbol{V}(t) + \boldsymbol{\omega} \times \boldsymbol{R}, \quad \boldsymbol{\omega} = \omega \cdot \boldsymbol{i}, \\ &\boldsymbol{R} = -R \cdot \boldsymbol{\Delta} / \Delta. \end{aligned} \qquad (14)$$

Here $\boldsymbol{R}$ is a radius vector connecting the center of the rotor and the contact point.

Slip speed $\boldsymbol{V}_T$ is directed tangentially to the rotor at the contact point and could be derived by subtracting from (14) the part which is orthogonal to contact surface:

$$\begin{aligned} &\alpha = (\boldsymbol{V}_P(t) \cdot \boldsymbol{\Delta}) / \Delta^2, \\ &\boldsymbol{V}_T(t) = \boldsymbol{V}_R(t) - \alpha \cdot \boldsymbol{\Delta} = \boldsymbol{V}(t) + \boldsymbol{\omega} \times \boldsymbol{R} - \alpha \cdot \boldsymbol{\Delta}. \end{aligned} \qquad (15)$$

Taking into account expressions (11), (12) and (15) for the vector of tangential contact force, we can get:

$$\boldsymbol{T} = -\mu \cdot N \cdot \boldsymbol{\tau}, \quad \boldsymbol{\tau} = \boldsymbol{V}_T(t) / |\boldsymbol{V}_T(t)|.$$

Here $\mu$ is the coefficient of sliding friction.

Thus, we define the formula for the force effecting the rotor at the contact point with the retainer bearing:

$$\boldsymbol{F} = \boldsymbol{N} + \boldsymbol{T}, \quad F_y = N_y + T_y, \quad F_z = N_z + T_z. \qquad (16)$$

The force (16) with point of application in the cross-section with coordinate $x=x_u$ is accounted for in the discrete model of dynamics of the rotor (4) by the vector of the generalized forces:

$$\begin{aligned} &\boldsymbol{R}_a = F_y \cdot \boldsymbol{U}_0^T, \quad \boldsymbol{R}_b = F_z \cdot \boldsymbol{U}_0^T, \\ &\boldsymbol{U}_0 = (U_1(x_u), ..., U_K(x_u)). \end{aligned}$$

Expressions (11), (12) are elementary linear dependencies of forces from speeds and deformations of interacting surfaces. The methods used in this paper for accounting for such forces in the mathematical model (4) were previously applied for cases that are more complex (for example, see [12]), so they are easily applied here.

The tangential component of the contact force (16) creates braking torque $M_T = T\,R$ directed at rotation axis. Angular speed of the rotor is defined by

$$I \frac{d\omega}{dt} = M_B - M_C - M_T, \qquad (17)$$

Here $I$ is the axial moment of inertia, $M_B$ is the turning moment and $M_C$ is the moment of resistance.

*D. The control system*

The force $F_m$ effecting the rotor from the magnet is defined as derivative of magnetic energy concentrated in the clearing between electromagnet coil and the rotor by the rotor displacement [13]. The force depends on the rotor displacement $Y_R$ and on the current $I_m$ flowing through the coils of the magnet. The current on its turn depends from the control voltage $U_m$ supplied to the coils of the AMB magnet and on its inductance $L$ and ohmic resistance $R$:

$$\begin{aligned} &F_m = G_m \frac{L_0 S_0}{2} \left( \frac{I_m}{S_0 - Y_R} \right)^2; \quad L = \frac{L_0 S}{S - Y_R}; \\ &\Psi_m = L I_m; \quad \frac{d\Psi_m}{dt} + R I_m = U_m. \end{aligned}$$

Here $L_0$ is the inductance of the coils of the magnet when the rotor is centered. $\Psi_m$ is *full* magnetic flux (magnetic linkage) in the magnet coils. $G_m$ is the coefficient, which depends on the AMB design and materials used. $S$ is the effective (magnetic) clearance, which defines the dependency of inductance of the coils of the magnet from the displacement of the rotor. $S_0$ is the effective clearance, which defines the dependency of the force effecting the rotor from the coils of the magnet from the displacement of the rotor.

The control system's task is to govern the control voltage being supplied to the coils of the magnet.

Initial information used by the control system are the displacements of the rotor $Y_d$ in the sections where sensors are located. The displacements of the rotor are converted to the displacement signal $Y_s$ taking into consideration sensors response time $T_1$:

$$T_1 \frac{dY_s}{dt} + Y_s = Y_d.$$

The displacement signal is defined by the sequence $Y_k$ – sensors being measured periodically with displacement sensors' measuring period $T_2$:

$$Y_k = Y_s(t_k), \; t_k = t_0 + kT_2, \; k = 0, 1, 2, .... \qquad (18)$$

Here $t_0$ is time delay used to account for nonsimultaneous measurements of the sensors of different AMB.

The sequence (18) is the starting information for generation of the mismatch current $I^*$ and the control current $I_{cc}$. When using PID control

$$\begin{aligned} &I^*(t) = A_{pr} Y_{k-1} + B_{dif}(Y_{k-1} - Y_{k-2})/T_2 + \\ &+ C_{int} T_2 (Y_{k-1} + Y_{k-2}, + ...), \; t_k < t < t_{k+1}. \end{aligned}$$

$$I_{cc} = I_0 + I^* \text{ or } I_{cc} = I_0 - I^*.$$

Here $A_{pr}$, $B_{dif}$ and $C_{int}$ are proportional, differential and integral control parameters; $I_0$ is rated operating current in the coils of the magnet.

The control current is constrained:

*if* $I_{cc} > I_{max}$ *then* $I_{cc} = I_{max}$ ;

*if* $I_{cc} < 0$ *then* $I_{cc} = 0$.

Here $I_{max}$ is the maximum allowed current in the coils of AMB electromagnet.

The control current is the starting information for generation of the control voltage $U_m$ being supplied to coils of the magnet. The control voltage can have one of the three possible values: $0$, $+U_{max}$, $-U_{max}$.

The algorithm for generating the control voltage is given below.

*Turning on (setting $U_m$ to either $+U_{max}$ or $-U_{max}$):*

*if $R_{fb}*(I_m - I_{cc}) < -\Delta U$ then $U_m = +U_{max}$.*

*if $R_{fb}*(I_m - I_{cc}) > +\Delta U$ then $U_m = -U_{max}$.*

*Turning off (setting $U_m$ to 0):*

*if $U_m = +U_{max}$ and $R_{fb}*(I_m - I_{cc}) > +\Delta U$ then $U_m = 0$.*

*if $U_m = -U_{max}$ and $R_{fb}*(I_m - I_{cc}) < -\Delta U$ then $U_m = 0$.*

Here $R_{fb}$ is the feedback factor measured in Ohms. $\Delta U$ is the factor describing the dead zone of the control system.

Therefore, in the model of the control system of AMB we have accounted for the following main factors, degree of influence of which is to be numerically and experimentally studied:

- Nonlinear dependency of the electromagnetic forces from the current in the coils of the AMB magnet and from the displacements of the rotor;
- Difference between the coordinates of the sensors and their respective AMB;
- Inertia of the electromagnets;
- Discrete nature of reading of the rotor displacement sensors;
- Time delay between generation of the control voltage and its supply to the coils of the AMB magnets;
- Dead zone and hysteresis presence in the control system;
- Limited maximum currents in the AMB coils.

### *E. Controlling the forces generated by AMB*

The model also allows simulating the ability to control the forces from AMB magnets. Nominally, the problem of controlling the AMB force is reduced to generation of the current $I_{cc}$ in the magnets which, when flowing through the coils, generates the force $F$ that obeys desired control law. The force $F$ depends on the current in the magnets and on the rotor displacement in the cross-sections where AMB are located:

$$F = \Phi(I_{cc}, y) \qquad (19)$$

Specific function $\Phi(I_{cc}, y)$ is defined by the design of the magnets and the rotor and could be found numerically or experimentally. With (19) known we can express the current as function of the rotor displacement and AMB force:

$$I_{cc} = \Psi(y, F) \qquad (20)$$

Given measured displacements $y$ the current generated in the coils of the AMB according to (20) will lead to generation of the desired force by AMB magnets.

Let us consider the algorithm for generating the control current for known dependency of AMB magnet forces from the currents in the magnet coils and from the rotor displacement [13]:

$$F = \begin{cases} C\dfrac{(I_0 - I_{cc})^2}{(S_0 - y)^2}, & I_{cc} \le -I_0 \\ C\left[\dfrac{(I_0 - I_{cc})^2}{(S_0 - y)^2} - \dfrac{(I_0 + I_{cc})^2}{(S_0 + y)^2}\right], & -I_0 < I_{cc} < I_0, \quad C = \dfrac{L_0 S_0}{2}. \\ -C\dfrac{(I_0 + I_{cc})^2}{(S_0 + y)^2}, & I_{cc} \ge I_0 \end{cases} \qquad (21)$$

Here $L_0$ is the magnet coils inductance; $S_0$ is the rated clearance between the rotor and the AMB magnets; $I_0$ is prespecified constant current in the coils.

From (21) we can derive the dependency of the control current form the rotor displacement and AMB force (20):

$$I_{cc} = \begin{cases} -I_0 + (S_0 + y)\sqrt{-\dfrac{F}{C}}, & F \le -\dfrac{4CI_0^2}{(S_0 + y)^2}, \\ \dfrac{1}{2S_0 y}\left[I_0(S_0^2 + y^2) - (S_0^2 - y^2)\sqrt{I_0^2 + yS_0\dfrac{F}{C}}\right], & -\dfrac{4CI_0^2}{(S_0 + y)^2} < F \le \dfrac{4CI_0^2}{(S_0 - y)^2}, \\ I_0 - (S_0 - y)\sqrt{\dfrac{F}{C}}, & F \ge \dfrac{4CI_0^2}{(S_0 - y)^2}. \end{cases} \qquad (22)$$

Second line here corresponds to the case of $y \neq 0$. When $y \approx 0$ it is reduced to $I_{cc} = -S_0^2 F/(4CI_0)$ by substituting (21).

By utilizing the expression (22) we can set the desired law of dependency of electromagnetic force $F$ from the rotor displacement.

## III. NUMERICAL STUDIES

To confirm the correctness of the assumptions upon which the computer model of dynamics of the rotor on electromagnetic suspension is based we used experimental data obtained from special stand. The stand has vertical heterogeneous rotor on one axial and two radial active magnetic bearings having common control system. Rotor weight is about 7.5 kg, length is about 0.75 m. Rated clearance between the rotor and the stator in the axial AMB is 0.45 mm, in the radial AMB 0.3 mm.

Figures 2 (experimental data) and 3 (numerically calculated data) depict the results of hanging out nonrotational rotor on the axial AMB starting from the lowest position.

Figure 4 depicts outer borders of the stability region on the plane formed by proportional (axis $A_{pr}$) and differential (axis $B_{dif}$) coefficients of PID control of radial AMB for the case when all the AMB have the same coefficients. In the stability region nonrotational rotor is guaranteed to move without contacting the retainer bearings.

Figure 5 depicts acceleration of the rotor from 0 rpm to 3600 rpm ($A_{max}$ is the maximal amplitude of the rotor displacement in the upper radial AMB).

Figures 3 and 4 have thin lines connecting numerical data while bold ones connect experimental data.

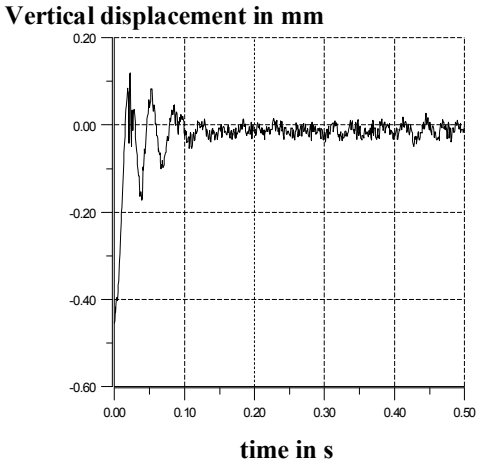


Figure 2. Experimental vertical displacements of the rotor when hanging out on axial AMB from the lowest position.

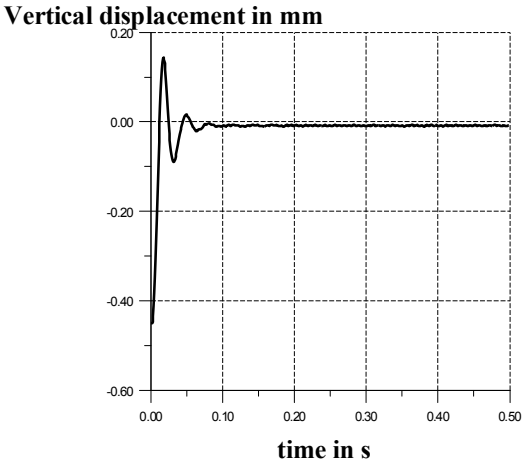


Figure 3. Numerically calculated vertical displacements of the rotor when hanging out on axial AMB from the lowest position.

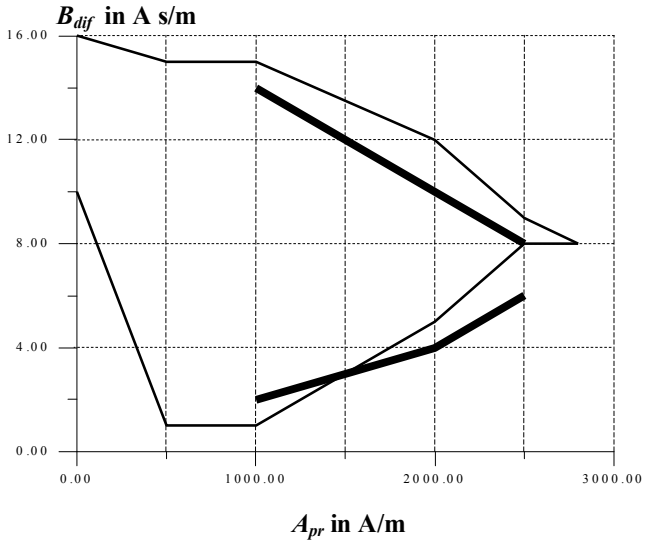


Figure 4. Borders of the stability range for radial AMB for the nonrotating rotor.

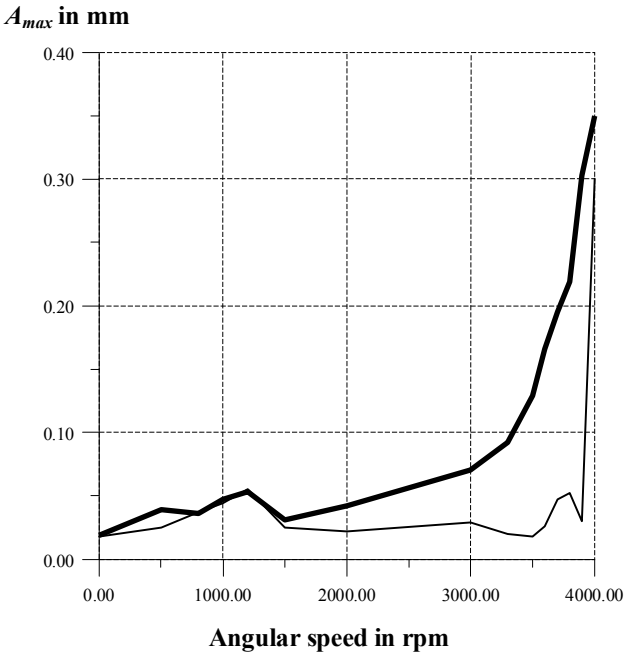


Figure 5. Acceleration of the rotor. $A_{max}$ is the maxial amplitude of the rotor displacement in the upper radial AMB

The difference between numerical and experimental data in the range of high frequencies is caused by the presence of residual imbalance.

The comparison of the results shown above as well as in verification studies [14, 15] proves the correctness of the core assumptions used to design the computer model.

Numerical experiments for emergency modes were performed for experimental stand RSM (Rotor Scale Model) [16] (Figure 6). RSM is composed by two rotors: the generator one and the turbocompressor one which are connected by the elastic clutch. Each rotor is supported by two radial and one axial AMB. RSM mass is around 1000 kg and length around 10 m. Radial AMB retainer bearing radii are from 40 to 50 mm, clearance between the rotor and the stator in all the retainer bearings is the same and equals to 0.4 mm.

We have modelled the malfunctions caused by imbalance changes, structural deviations of the rotor and by control system failures.

Numerical experiments were conducted for different imbalance configurations. In the first case imbalance radii are the same for all rotor elements and imbalance directions are also the same (one-sided imbalance). In the second case imbalance directions are different (multidirectional imbalance).

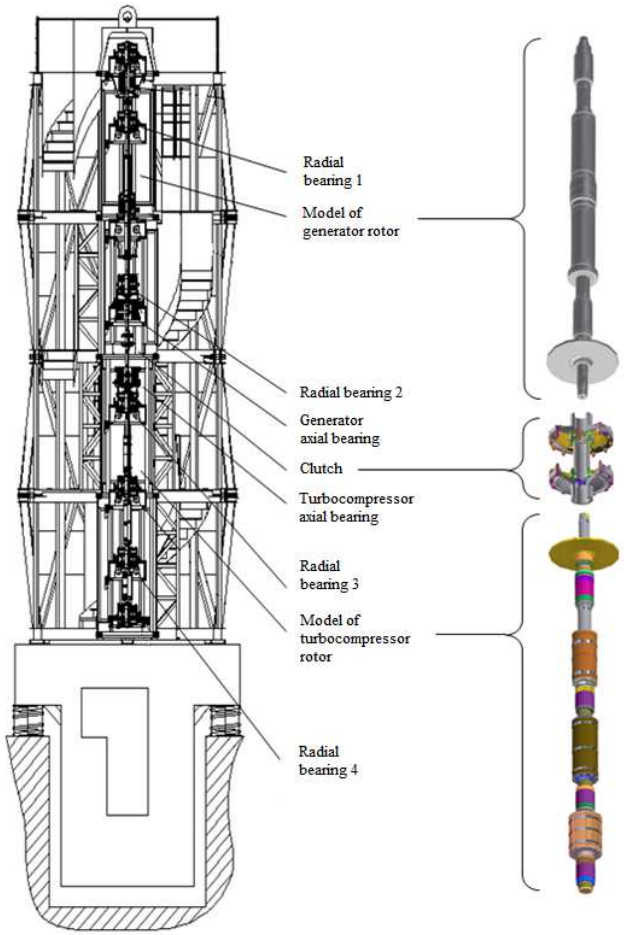


Figure 6. Experimental stand of the Rotor Scale Model [16] of High-Temperature Gas-Cooled Reactor [1]

Table 1. Amplitudes (in microns), corresponding to frequency of 60 Hz, in radial AMB of RSM.

| | AMB 1 | AMB 2 | AMB 3 | AMB 4 |
|---|---|---|---|---|
| One-sided imbalance in the RSM rotor | 9 | 8 | 9 | 10 |
| Changed imbalance in the generator rotor | 13 | 6 | 9 | 10 |

Oscillation spectrum deformation was observed in radial AMB of the generator rotor of RSM. In the AMB 1 oscillations amplitude corresponding to rotation frequency of 60 Hz became half again as many (see Table 1).

We have also studied possible malfunctions related to change in rigidity of individual elements of the rotor. We assumed that failing element of the rotor changes to have a spring linkage with its rigidity changing from $10^8$ N m to $10^3$ N m.

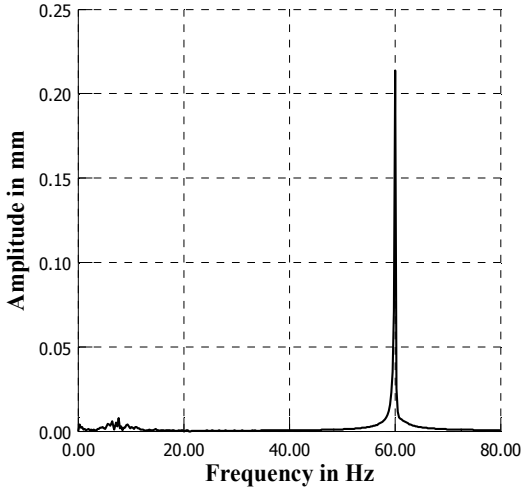


Figure 7. Spectrum in the AMB 2 when rigidity changes to 1000 N m.

Figure 7 depicts the spectrum of the rotor oscillations in the AMB 2. When rigidity is changed due to presence of the imbalance the amplitude of the oscillations increases tenfold on the rotation frequency of 60 Hz.

Table 2. Amplitudes (in microns), corresponding to frequency of 60 Hz, in radial AMB of the generator of RSM.

| | AMB 1 | AMB 2 |
|---|---|---|
| Initial rigidity | 26 | 17 |
| Changed rigidity | 34 | 213 |

We have also studied the case of failure of the control system leading to no generation of the force in one of the radial AMB (Figure 8 and 9).

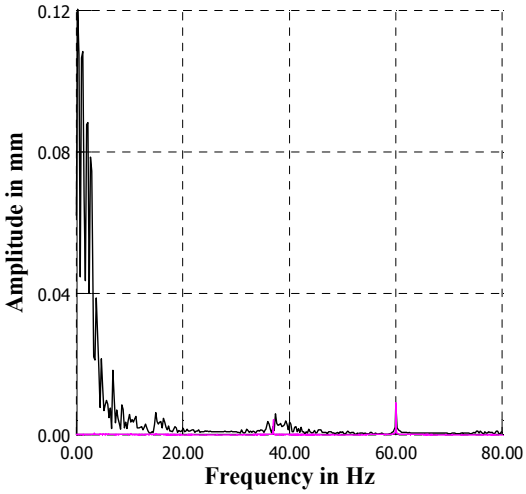


Figure 8. Change of the spectrum in the AMB 1 of RSM due to its force missing along the radial direction 0*y*; magenta curve is initial spectrum; black curve is disturbed spectrum.

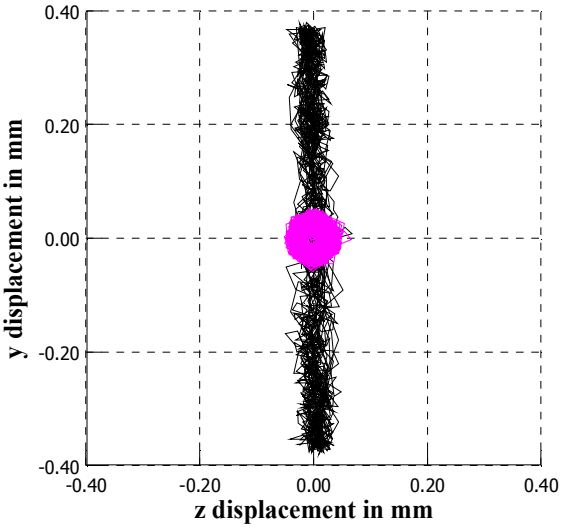


Figure 9. The trajectory of oscillations of the generator rotor of RSM in AMB 1; magenta curve is before the failure, black curve is after failure.

Due to interaction with the retainer bearing along the 0*y* axis in the AMB 1 the oscillations have maximum amplitude. The frequency in this case shifts to lower range with appearance of "rattling".

## IV. CONCLUSION

We have developed the computer model of dynamics of a multispan flexible rotor on AMB and applied it for composing of diagnostic characters of malfunctions caused by: imbalance change, rigidity change in one of the rotor elements, change of the control system parameters. Conducted numerical experiments show the possibility to define the malfunction signatures needed by the diagnostic system using the developed computer model.

## V. ACKNOWLEDGEMENT

The research was performed with financial support from Russian Science Fund (Grant No. 16-19-10279).

## REFERENCES

[1] F. M. Mitenkov, N. G. Kodochigov, et al., "Hightemperature gas-cooled reactors - energy source for industrial production of hydrogen," *Atomic Energy*, vol. 97-6, pp. 432-446, 2004.

[2] N. X. Wang, J. G. Zhang, G. P. Ding, "Influence of Magnetic Bearing Stiffness on Rotor in Wind Turbine Generator," *Applied Mechanics and Materials*, Vol 150, P. 57-62, Jan. 2012.

[3] F. M. Mitenkov, A. S. Chistov, V. F. Ovchinnikov, M. Ya. Nikolaev, E. V. Kiryushina, V. N. Litvinov, E. V. Fadeeva, O. G. Savikhin, "Electromagnetic Suspension in Vertical Axial Wind-Driven Generators," *Journal of Machinery Manufacture and Reliability*. 2015r. Vol.44. No3. P.195–199.

[4] F. M. Mitenkov, V. V. Znyshev, E. F. Sabaev, L. V. Smirnov, A. L. Prigorovskij, "Problems and principles of mathematical simulation of complex unique system dynamics," *Matem. Mod.*, vol. 19-5, pp. 39-44, 2007.

[5] F. M. Dimentberg, K.S. Kolesnikov et al, "Vibrations in engineering. Handbook in 6 volumes.Vol. 3. Oscillations of machines, structures and their elements," Moscow, *Mashinostroenie publishers*, 1980.

[6] S. Timoshenko, D. H. Young, and W. Weaver, Jr., "Vibration Problems in Engineering," New York, Chichester, Brisbane, Toronto, Singapore, *John Wiley & Sons*, 1974.

[7] M. Kandil, "On Rotor Internal Damping Instability," PhD Thesis, *University of London*, 2004.

[8] G. S. Pisarenko, "Oscillations of mechanical systems accounting for imperfect rigidity of material," Kiev, *Naukova dumka publishers*, 1970.

[9] E. S. Sorokin, "About inner damping theory applied for oscillation of flexible systems," Moscow, *Gosstroyizdat publishers*, 1960.

[10] Ya. G. Panovko, "Inner damping in flexible systems oscillations," Moscow, *Physmatgiz publishers*, 1960.

[11] I. V. Burmistrov, A. V. Kozin, V. F. Ovchinnikov, V. A. Panov, L. V. Smirnov, "Modeling the static and dynamic deformations of pipeline systems on supports with nonlinear characteristics," *Problems of Strength and Plasticity,* issue 71, 2009, pp. 95-103.

[12] A. N. Nikiforov, "Generalized mathematical model of a Jeffcot-Laval rotor taking into account slipping during contact and misaslignment with stator," *Bulletin of Science and Technical Development*, issue 5, vol. 57, 2012, pp. 41-56.

[13] G. Schweitzer, E. H. Maslin et al, "Magnetic bearings in engineering," Dordrecht, Heidelberg, London, New York, *Springer*, 2009.

[14] V. F. Ovchinnikov, M. Ya, Nikolaev, V. N. Litvinov, "Algorithm for Accounting for Inner Damping in a Computer Model of Dynamics of a Flexible Rotor on Active Magnetic Bearings," *ACES Journal*, vol. 32, issue 8, 2017, pp. 726-730.

[15] V. F. Ovchinnikov, M. Ya. Nikolaev, V. N. Litvinov, N. G. Kodochigov, I. V. Drumov, "Accounting for structural deviations in the model of dynamics of a rotor on complete electromagnetic suspension," *Thermal Engineering,* vol. 65, issue 9, 2018, to be published.

[16] I. V. Drumov, N. G. Kodochigov, S. E. Belov, D. S. Znamensky, C. B. Baxi, A. Telengator, J. Razvi "Studies of the Electromagnetic Suspension System for the GT-MHR Turbo Machine Rotor Model," *Proceedings of HTR 2010*. Prague, Czech Republic, October 18–20, no. 41. pp. 1–7, 2010.